

## Article

# Gravity Separation Tests of a Complex Rutile Ore

Zhenxing Wang<sup>1,2</sup>, Yongxing Zheng<sup>1,2,\*</sup>, Xiang Huang<sup>3</sup>, Xiangding Wang<sup>3</sup>, Jieli Peng<sup>1,2</sup> and Zhe Dai<sup>1,2</sup>

- <sup>1</sup> State Key Laboratory of Complex Nonferrous Metal Resources Clean Utilization, Kunming University of Science and Technology, Kunming 650093, China; wangzhenxing0826@126.com (Z.W.); a18308247896@163.com (J.P.); daiz410@163.com (Z.D.)
- <sup>2</sup> Faculty of Land Resource Engineering, Kunming University of Science and Technology, Kunming 650093, China
- <sup>3</sup> Guangdong Ubridge New Material Technology Co., Ltd., Maoming 525000, China; huangxiangbest@163.com (X.H.); 15766064624@126.com (X.W.)
- \* Correspondence: yongxingzheng2017@126.com

**Abstract:** The complex rutile ore containing TiO<sub>2</sub> and ZrO<sub>2</sub> exhibited a high economical value. To effectively recover TiO<sub>2</sub> and ZrO<sub>2</sub> from the raw sample, a complete gravity separation process including a spiral chute and a shaking table was proposed. Chemical constituents, phase, liberation degree and size distribution were firstly characterized by XRF, chemical analyses, XRD, EPMA-EDS and screening to understand the mineralogy. Then, two stages of spiral chute separation tests were performed to treat the complex rutile ore. A rough zircon concentrate containing 33.18% ZrO<sub>2</sub> was obtained after the first-stage spiral chute and a rough rutile concentrate containing 56.77% TiO<sub>2</sub> was obtained after the second-stage spiral chute. To further improve the grade and recovery of ZrO<sub>2</sub> and TiO<sub>2</sub> in the rough products obtained by spiral chutes, shaking table tests were performed. A zircon concentrate containing 42.65% ZrO<sub>2</sub> and a rutile concentrate containing 61.75% TiO<sub>2</sub> were obtained. For the tailing of the first-stage spiral chute, a rutile product assaying 57.50% TiO<sub>2</sub> was obtained, and the tailing was directly discarded as waste after the shaking table tests. Moreover, the distribution regularities of ZrO<sub>2</sub> and TiO<sub>2</sub> in the products were further revealed by XRD analyses. Finally, a closed-circuit beneficiation process was proposed to treat the complex rutile ore for achieving comprehensive and effective utilization.



**Citation:** Wang, Z.; Zheng, Y.; Huang, X.; Wang, X.; Peng, J.; Dai, Z. Gravity Separation Tests of a Complex Rutile Ore. *Minerals* **2024**, *14*, 68. <https://doi.org/10.3390/min14010068>

Academic Editors: Ozan Kokkilic, Pengbo Chu and Firat Burat

Received: 29 November 2023

Revised: 23 December 2023

Accepted: 27 December 2023

Published: 5 January 2024

**Correction Statement:** This article has been republished with a minor change. The change does not affect the scientific content of the article and further details are available within the backmatter of the website version of this article.



**Copyright:** © 2024 by the authors. Licensee MDPI, Basel, Switzerland. This article is an open access article distributed under the terms and conditions of the Creative Commons Attribution (CC BY) license (<https://creativecommons.org/licenses/by/4.0/>).

**Keywords:** complex ore; rutile; zircon; mineralogy; spiral; shaking table

## 1. Introduction

Titanium possesses good physical and chemical properties, including high mechanical strength, temperature resistance, corrosion resistance and strong reducibility [1,2]. Therefore, titanium metal and its various derivatives are widely used in aerospace, biomedicine and marine engineering. They are also indispensable metal materials for modern industry and cutting-edge technology [3–6]. Titanium metal is mainly extracted from titanium ore. The world's titanium ore resources are concentrated in more than 40 countries around the world and is distributed in the seven continents except Antarctica [7]. Titanium deposits are mainly divided into magmatic and hydrothermal deposits, and metamorphic deposits and sedimentary deposits according to their genetic types. Titanium minerals mainly include rutile, ilmenite, anatase and brookite [8].

The ilmenite and rutile are the main subjects in the global development and utilization of titanium ores. Among them, 98% of rutile and 30% of ilmenite are derived from valuable heavy minerals in placer deposits. Rutile is usually associated with zircon and monazite in deposits, and both of which are mostly used as by-products of titanium mineral processing [9,10]. Zircon and monazite are widely applied in the metallurgical industry, ceramics production and petrochemicals due to their unique physicochemical properties [11–13]. Australia, as a major producer of titanium products, has always been at the forefront of the

world in the processing of titanium resources, especially for the production of rutile, for it which ranks first [14,15]. Rutile deposits in Australia are mostly coastal placer deposits [16]. The valuable heavy minerals in the deposit are mainly rutile, ilmenite, zircon and monazite.

There are many processes, including gravity separation, magnetic separation and electrostatic separation, to recover valuable heavy minerals from the coastal sands [17,18]. N. Babu et al. [19] investigated a low content of red sand containing ilmenite and zircon from Tamil Nadu, India. The results showed that three products including ilmenite, zircon and silica were obtained after spiral chute, magnetic separation and electric separation. Rajan Girija Rejith et al. [20] reported the recovery of heavy minerals from the KV and KS areas, India, by multiple physical separation technologies. The findings revealed the presence of not only ilmenite but also monazite, zircon, and silica in the product of heavy minerals. Moumar Dieye et al. [21] separately used magnetic separation and gravity separation, to separate monazite from the rough zircon concentrate in Senegal. It was found that the recoveries of monazite were 94.8% and 76.6%, respectively, when magnetic separation and gravity separation were separately carried out. M M Fawzy et al. [22] recovered valuable heavy minerals from the southern coast of the Red Sea by shaking table, followed by magnetic separation. The results presented that the recoveries of heavy minerals reached 91.68%, 71.67% and 82.06%, respectively from three different areas.

However, there are few reports on complex rutile placer deposits. The sample studied in this paper was a complex rutile placer, which is a middling of dry electric separation of a seaside placer in Australia and was recycled by China Yueqiao New Materials Technology Co., Ltd., (Maoming, China). The company is committed to the production of rutile products with  $\text{TiO}_2$  grade of 70%–95% and zircon products with  $\text{ZrO}_2$  grade of 60%–66%. Among them, rutile products with  $\text{TiO}_2$  grade of 70%–90% are used in the downstream welding industry, rutile products with  $\text{TiO}_2$  grade of 90%–95% are used to produce titanium dioxide and zircon products with  $\text{ZrO}_2$  grade of 60%–66% are basically used in the manufacture of ceramics. The current procedure employed by the company involves magnetic separation, multistage shaking table, and electrostatic separation. However, the wet separation component has a limited processing capacity, and it is difficult to obtain high-grade concentrate, which increases the pressure of subsequent electrostatic separation.

The objective of this paper is to find a method for efficient separation of complex rutile ore in gravity separation, which can effectively separate and purify the target minerals in the gravity separation process, further improve the grade of the concentrate, provide high-quality raw materials for the electrostatic separation and reduce the pressure of the electrostatic separation. As is widely known, the processing capacity of a spiral chute is larger than that of a shaking table, but it is difficult to fine-tune the operation, while the shaking table has the characteristics of stable operation and is easy to fine-tune. Therefore, through the spiral chute–shaking table configuration, the processing capacity of gravity separation can be further increased while ensuring the increase in the grade of gravity separation concentrate. Mineralogy of the raw sample was firstly studied by chemical analyses and physical characterization to predict the separation performances. Then, a spiral chute was used to separate zircon and Ti-bearing minerals, followed by the use of a shaking table to obtain a wet concentrate with a high  $\text{ZrO}_2$  or  $\text{TiO}_2$  grade. Finally, a closed-circuit process was proposed based on the open-circuit process combining with experimental results.

## 2. Materials and Methods

### 2.1. Materials

The rutile middling was provided by the Yueqiao New Material Technology Co., Ltd., (Maoming, China). The results of X-ray fluorescence (XRF) analyses and chemical multi-element analyses are shown in Tables 1 and 2, respectively.

From Table 1, it is observed that the main elements in the sample were O, Si, Ti, Fe and Zr, accounting for 38.56%, 15.26%, 23.78%, 5.62% and 5.24%, respectively. From Table 2, the contents of  $\text{TiO}_2$  and  $\text{ZrO}_2$  assayed 33.78% and 5.56%, respectively, indicating that it was a

Ti-bearing middling sample which was associated with Zr-bearing minerals. In addition, the contents of  $\text{SiO}_2$  and  $\text{Al}_2\text{O}_3$  assayed 34.74% and 7.97%, respectively, indicating that considerable amounts of gangue minerals existed.

**Table 1.** XRF analyses of the rutile ore (%).

O	Na	Mg	Al	Si	P	S	Cl
38.36	0.05	0.25	2.75	15.26	0.02	0.04	0.02
Pb	U	Ca	Ti	Cr	Mn	Fe	Zn
0.03	0.01	0.10	23.78	0.07	0.12	5.62	0.04
Th	Zr	Nb	La	Ce	Nd	Hf	Y
0.14	5.24	0.07	0.24	0.47	0.20	0.17	0.07

**Table 2.** Chemical multi-element analyses of the rutile ore (%).

$\text{TiO}_2$	$\text{ZrO}_2$	Fe	$\text{Al}_2\text{O}_3$	$\text{SiO}_2$
33.78	5.56	5.72	7.97	34.74

## 2.2. Experimental Method

The general flow sheet for processing the raw sample is shown in Figure 1. About 20.0 kg of the raw sample was mixed with water in a ratio of 1:3 to obtain a pulp concentration of 25%. The pulp was fed into the first-stage spiral chute with a diameter of 1250 mm and a distance of 720 mm at a feed rate of 0.517 t/h by a circulating pump. As soon as the obvious distribution zones of products appeared, the products including rough zircon concentrate, rough rutile product and tailing I were separately obtained. The rough rutile product with a pulp concentration of 25% was fed into the second-stage spiral chute with a diameter of 1250 mm and a spacing of 720 mm through a circulating pump at a feed rate of 0.484 t/h to obtain a rough rutile concentrate and middling I.

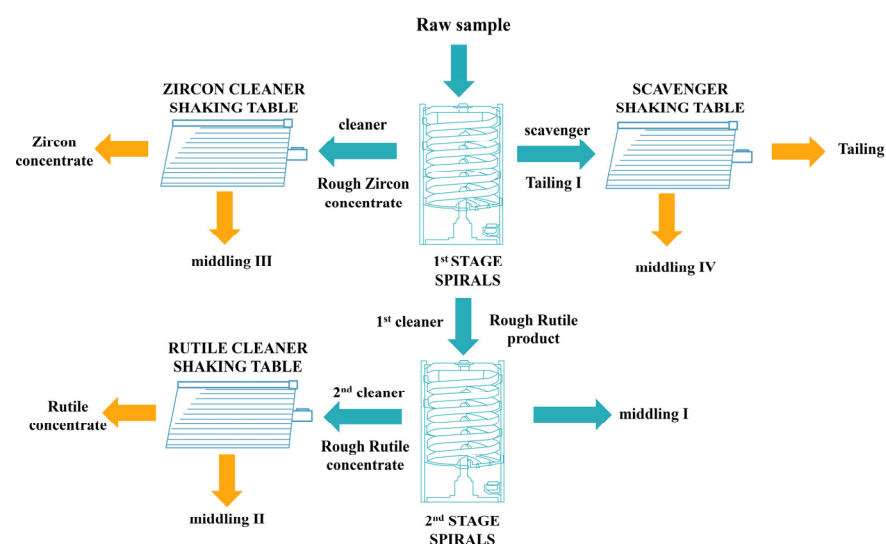


**Figure 1.** Flow chart of gravity separation tests.

The rough rutile concentrate entered the shaking tables and then the rutile concentrate and middling II were produced. The rough zircon concentrate was fed into the shaking tables and then the zircon concentrate and middling III were produced. The tailing I was fed into the shaking tables and then the middling IV and final tailing were produced. The final tailing was directly discharged as solid waste. The shaking tables were carried out

under these conditions: dimensions of 1100 mm × 500 mm, speed set at 350 rpm, deck inclination at 2°, and a stroke length of 10 mm.

### 2.3. Analytical Techniques

Constituents of the ore and contents of major elements tested by XRF analyses and chemical multi-element analyses, respectively. Phases of minerals were analyzed by using an X-ray diffraction analyzer (D/MAX 2200, Rigaku, Japan) with a voltage of 40 kV, a tube current of 40 mA, a swept surface range of 10°–90° and a swept surface speed of 5°/min. Mineral surface morphology and elemental contents were detected by using an XA-8230 Electron Probe Microanalyzer (EPMA). The probe currents were set to the range of 250 nm–500 nm and the accelerating voltage was fixed at 20 kV.

## 3. Results and Discussion

### 3.1. Mineralogical Characterization

#### 3.1.1. XRD Analyses

Figure 2 shows the XRD result of the raw sample. It is observed that the valuable metal minerals mainly included rutile and zircon and the gangue mineral was mainly quartz. The intensity of diffraction peaks was low, indicating that the minerals have poor crystal structure, which confirmed that it was an altered coastal placer.

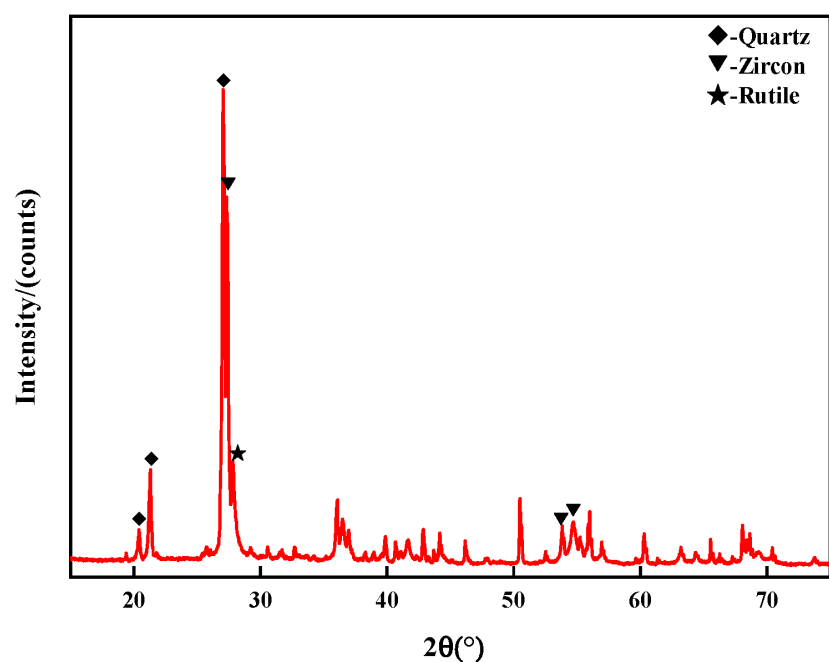
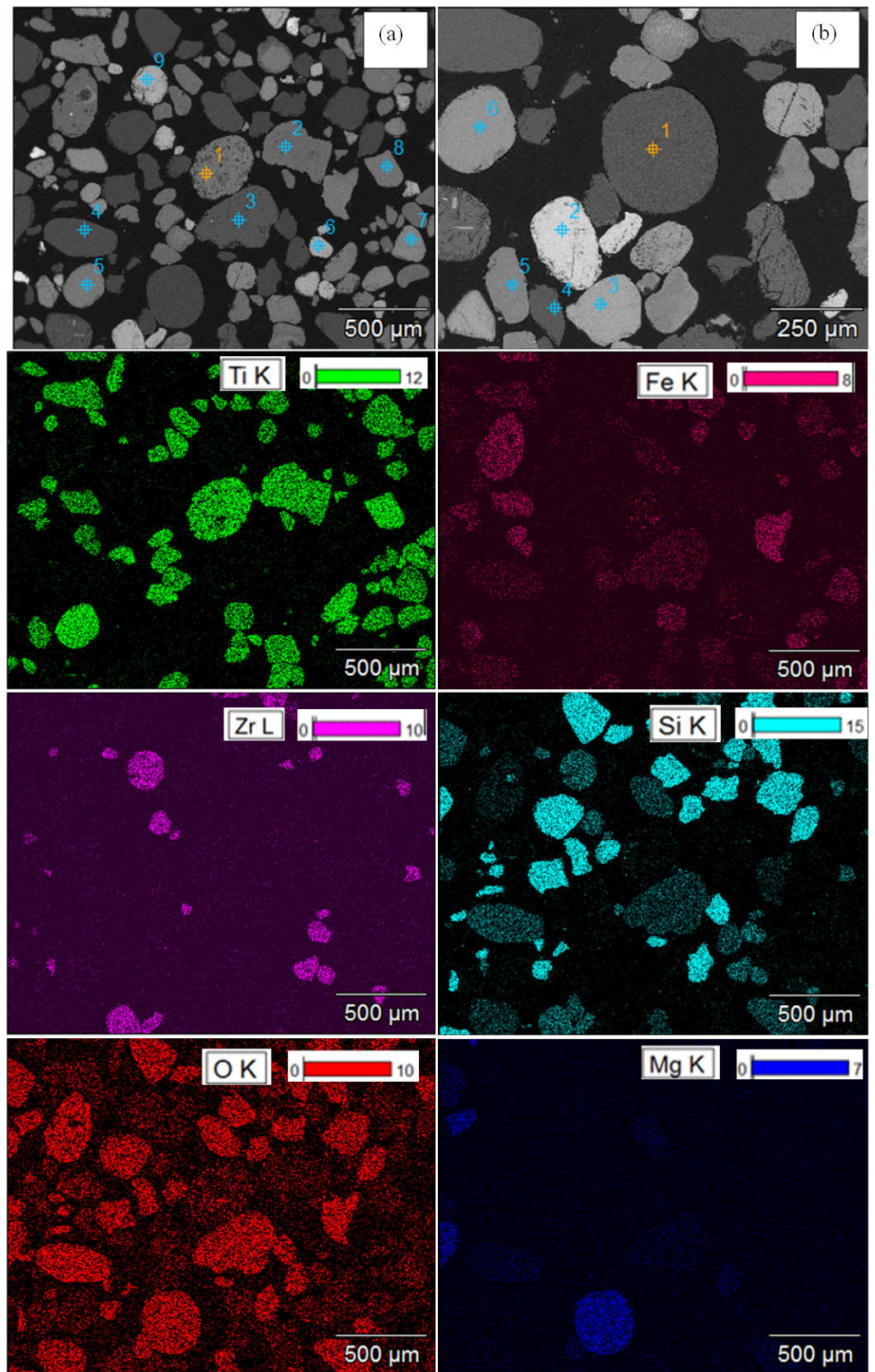


Figure 2. XRD pattern of the raw sample.

#### 3.1.2. EPMA-EDS Analyses

To investigate the mineral composition and distribution in the raw sample, EPMA analyses were carried out and the results are shown in Figure 3. From Figure 3a and the corresponding mapping, it is observed that signals of titanium, oxygen and even iron elements in particles which are located at points 1, 2, 5 and 8 completely coincided.



**Figure 3.** EPMA-EDS and mapping analyses results of the raw sample, (a) EPMA-EDS image, (b) an enlarged view of (a).

According to the EDS analyses results in Table 3, the particles at position 1, 2 and 5 were iron-containing rutile with an average iron content of 1.69%, while the particle at position 8 was rutile almost without iron. These results indicate that these particles were titanium oxide or iron-containing titanium oxide minerals. The signals of titanium, iron and oxygen elements in the particle which is located at point 7 completely coincided, which indicated that the particles at this position were ilmenite. The EDS analyses results in Table 3 further agreed with this deduction. The signals of zirconium, silicon and oxygen elements in particles 6 and 9 completely coincided, demonstrating that the particles were zircon. According to the results of EDS analyses in Table 3, it is known that particles which are located at points 3 and 4 were aluminosilicate minerals.

**Table 3.** EDS analyses results of the raw sample in Figure 3a (Weight %).

Point	O	Mg	Al	Si	Ti	Mn	Fe	Zr
1	36.97	-	0.29	-	61.55	-	1.19	-
2	35.78	-	0.87	-	60.91	-	1.46	-
3	44.73	1.49	28.48	13.44	0.33	-	11.52	-
4	48.13	3.01	18.93	18.13	0.28	-	9.46	-
5	35.10	-	-	-	61.80	-	2.43	-
6	32.30	-	-	15.70	-	-	-	52.00
7	33.04	-	-	-	38.05	2.18	26.73	-
8	30.72	-	-	-	69.28	-	-	-
9	31.26	-	-	15.62	-	-	-	53.12

Figure 3b is an enlarged view of Figure 3a and the corresponding EDS analyses results are shown in Table 4. The results further confirmed that the raw ore sample was composed of iron-bearing rutile (points 5 and 6), zirconite (point 2), ilmenite (point 3) and magnesium–aluminum spinel (point 1) and quartz (point 4).

**Table 4.** EDS analyses results of the raw sample in Figure 3b (Weight %).

Point	O	Mg	Al	Si	Ti	Mn	Fe	Zr
1	40.87	17.19	39.92	-	-	-	2.02	-
2	32.32	-	-	15.46	-	-	-	52.22
3	30.55	-	-	-	39.39	1.65	28.41	-
4	50.78	-	-	49.22	-	-	-	-
5	37.78	-	-	-	64.47	-	0.75	-
6	31.38	-	-	-	66.21	-	2.41	-

Considering the results of EPMA-EDS and mapping analyses, it was concluded that the rutile or zircon in the raw ore samples had a good degree of liberation.

### 3.1.3. Size Distribution

To determine the distribution of titanium and zirconium in different grain sizes of the raw sample, particle size analyses were carried out, as shown in Table 5. Titanium dioxide was mainly enriched in the particle size of  $-0.15$  mm and the distributions reached 95.17%. And zirconium dioxide was mainly enriched in the particle size of  $-0.106$  mm and the distribution reached 86.72%. It was further found that  $\text{TiO}_2$  was more evenly distributed in the fractions of  $-0.15\sim+0.106$  mm,  $-0.106\sim+0.074$  mm and  $-0.074$  mm, and the distribution of  $-0.074$  mm  $\text{TiO}_2$  was 32.08%.  $\text{ZrO}_2$  was mainly distributed in the fractions of  $-0.106\sim+0.074$  mm and  $-0.074$  mm, and the distribution of  $\text{ZrO}_2$  in  $-0.074$  mm was as high as 52.25%. It is obvious to observe that the valuable metal minerals were mainly distributed in fine particles and the proportion of rutile and zircon was similar, which undoubtedly increased the difficulty for recovering fine-grained valuable minerals.

**Table 5.** Results of particle size analyses.

Particle Size/mm	Yield/%	Grade/%		Distribution/%	
		TiO <sub>2</sub>	ZrO <sub>2</sub>	TiO <sub>2</sub>	ZrO <sub>2</sub>
+0.25	1.63	2.29	0.46	0.11	0.11
−0.25~+0.18	3.22	11.30	0.99	1.08	0.45
−0.18~+0.15	5.84	21.07	1.15	3.64	0.95
−0.15~+0.106	33.96	26.98	1.90	27.11	11.77
−0.106~+0.074	30.15	40.31	6.55	35.97	34.47
−0.074	25.19	43.03	13.55	32.08	52.25
Feeding	100.00	33.78	6.15	100.00	100.00

### 3.2. Spiral Chute Tests

#### 3.2.1. First-Stage Spiral Chute

Spiral chutes have been an extensive application in the treatment of heavy mineral sand deposits and even fine coal in recent years [23–25]. Ports for the separation of the higher specific-gravity particles are located at the lowest points in the cross section. The zone width of products which were removed at the port is controlled by adjustable splitters. Therefore, width of discharge port was especially investigated for the spiral chute, as shown in Figure 4. From Figure 4, it is observed that distribution zones of four products including rough zircon concentrate (A), rough rutile product (B), gangue (C) and slime (D) appeared. Factually, spiral chutes usually contain three discharge ports. So, gangue and slime were merged as tailing I. The formation of mineral zones are broadly divided into three stages. In the first stage, the heavy minerals gradually turn into the bottom layer, and the light minerals enter the upper layer when the mineral particles group moves along the bottom of the spiral chute. This stage will be basically completed after the first circle of spiral chute. In the second stage, both the light and heavy minerals are zoned along the lateral direction. The bottom-heavy minerals with small centrifugal acceleration move to the inner edge, and the upper light minerals move to the outer area of the middle, and the slime which is suspended in the water is thrown to the outermost ring. This stage lasts approximately until the last circle of the spiral chute. And the mineral particles with different specific gravity and particle size need different distances to reach a stable state of motion. In the third stage, the movement reaches a balance. The mineral particles with different properties move along their own semi-rotational motion to complete the separation process [26]. Consequently, the adjustable splitters are placed at the lowest point of the spiral chute, creating three discharge ports. The widths of the discharge ports for concentrate and middling and the results are shown in Table 6.

From Table 6, it is known that ZrO<sub>2</sub> grade in the rough zircon concentrate reached 33.62% with a recovery of 37.48%, while TiO<sub>2</sub> grade in the rough rutile product reached 40.50% with a recovery of 86.55% when the adjustable splitters were fixed at position I. When the splitters were adjusted to position II, recoveries of ZrO<sub>2</sub> in the rough zircon concentrate and TiO<sub>2</sub> in the rough rutile product increased to 62.43% and decreased to 72.16%, respectively, although ZrO<sub>2</sub> grade in the rough zircon concentrate slightly fluctuated and TiO<sub>2</sub> grade in the rough rutile product increased. With further adjusting the splitters to position III, ZrO<sub>2</sub> recovery in the rough zircon concentrate increased to 78.79%, whereas the grade decreased to 26.14%, which signified that the separation of zircon in the subsequent steps will be under a large pressure. Meanwhile, TiO<sub>2</sub> grade in the rough rutile product had little changes, but TiO<sub>2</sub> recovery decreased to 64.30%, which demonstrates that it was disadvantageous for the effective recovery of rutile. Therefore, the adjustable splitters were fixed as position II as the best testing position.

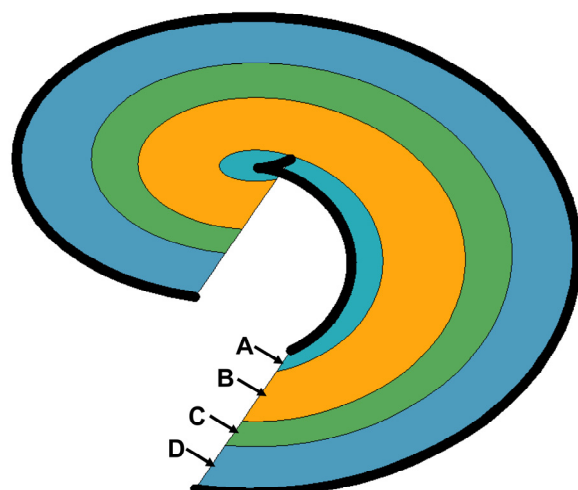


**Figure 4.** First-stage spiral chute distribution zones of products, A—rough zircon concentrate, B—rough rutile product, C—gangue, D—slime.

**Table 6.** Experimental results of the first-stage spiral chute.

Adjustable Splitter Position	Products	Yield/%	Grade/%		Recovery/%	
			TiO <sub>2</sub>	ZrO <sub>2</sub>	TiO <sub>2</sub>	ZrO <sub>2</sub>
Position I width of discharge port (5 cm; 9.5 cm)	A	6.50	24.04	33.62	4.75	37.48
	B	70.25	40.50	2.55	86.55	30.77
	Tailing I	23.25	12.30	7.96	8.70	31.74
	Feeding	100.00	32.88	5.82	100.00	100.00
Position II width of discharge port (7.2 cm; 4.5 cm)	A	10.74	27.13	33.18	8.72	62.43
	B	55.40	43.52	3.71	72.16	36.04
	Tailing I	33.86	18.86	0.26	19.11	1.52
	Feeding	100.00	33.56	5.72	100.00	100.00
Position III width of discharge port (8.7 cm; 3.5 cm)	A	16.68	36.13	26.14	17.98	78.79
	B	49.26	43.76	2.24	64.30	19.96
	Tailing I	34.06	17.45	0.20	17.73	1.25
	Feeding	100.00	33.53	5.54	100.00	100.00

### 3.2.2. Second-Stage Spiral Chute

According to Section 3.2.1, yield of the rough rutile product reached 55.40%, suggesting that large amounts of rutile entered the middling in the first-stage spiral chute. So, the second-stage spiral chute was continuously used to treat the rough rutile product. The width of discharge port was also studied, as shown in Figure 5. From the figure, it is observed that distribution zones of three products including rough rutile concentrate (E), gangue (F) and slime (G) appeared. To focus on the effects of discharge port on the indexes of rough rutile concentrate, gangue (F) and slime (G) were merged as middling I. Consequently, the adjustable splitters are placed at the lowest point of the spiral chute, creating two discharge ports. The widths of the discharge ports and the second-stage spiral chutes testing results are shown in Table 7.

From Table 7, it is seen that TiO<sub>2</sub> grade in the rough rutile concentrate reached 51.12% with a recovery of 77.82% when the adjustable splitters were fixed as position I. When the splitters were adjusted to position II, TiO<sub>2</sub> grade in the rough rutile concentrate increased to 56.77%, but the recovery of TiO<sub>2</sub> decreased to 63.35%. The higher the TiO<sub>2</sub> grade in the rough rutile concentrate was, the more favorable for the subsequent separation and purification. On the other hand, TiO<sub>2</sub> grade in the Middling I was closed to the feeding of the raw sample, that is, the Middling I can be returned to the feeding, forming a closed-



circuit system to increase the  $\text{TiO}_2$  recovery. Therefore, the adjustable splitters were fixed as position II as the best testing position.

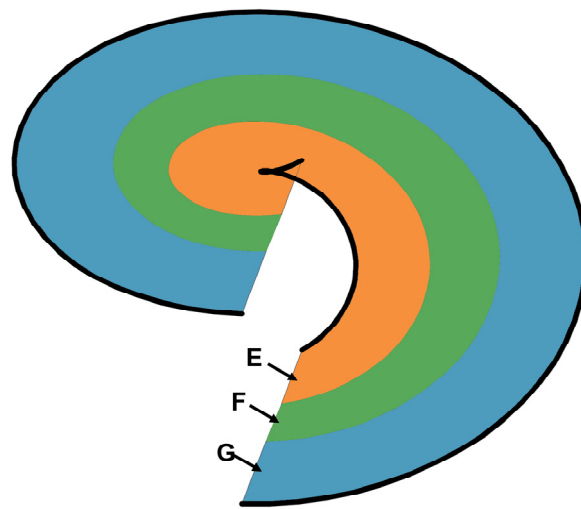


**Figure 5.** Second-stage spiral chute distribution zones of products, E—rough rutile concentrate, F—gangue, G—slime.

**Table 7.** Experimental results of the second-stage spiral chute.

Adjustable Splitter Position	Products	Yield/%	Grade/%		Recovery/%	
			$\text{TiO}_2$	$\text{ZrO}_2$	$\text{TiO}_2$	$\text{ZrO}_2$
Position I width of discharge port (7.5 cm)	E	67.91	51.12	4.53	77.82	84.01
	Middling I	32.09	27.92	1.65	22.18	15.99
	Feeding	100.00	43.68	3.54	100.00	100.00
Position II width of discharge port (5 cm)	E	47.64	56.77	4.64	63.65	63.23
	Middling I	52.36	31.30	2.46	34.45	36.77
	Feeding	100.00	43.43	3.50	100.00	100.00

### 3.3. Shaking Table Tests

#### 3.3.1. Tests for the Rough Zircon Concentrate

To further increase grade of the rough zircon concentrate, shaking table tests were performed in the laboratory and the results are shown in Table 8. From the table, it is seen that a mixed concentrate containing 42.65%  $\text{ZrO}_2$  was obtained and the recovery of  $\text{ZrO}_2$  reached 60.17%, indicating that the grade of  $\text{ZrO}_2$  in the rough zircon concentrate could be increased by further gravity separation. However, the losing recovery of  $\text{ZrO}_2$  in the tailing (Middling III) reached 39.83%, which may be accounted by the fact that considerable amounts of zircon have small size in the sample. Their own gravity of the fine particles could not overcome other forces which were offered by viscous fluid and mechanical vibration [27], resulting in the zircon entering the tailing. It was proposed that some special gravity separators such as grooving shaking table [28], rotary cone separator [29] and centrifugal machine [30] were adopted in the subsequent tests. Whatever equipment was used, the Middling III could be returned to the feeding of the second-stage spiral chute to further recover rutile and zircon.

**Table 8.** Results of shaking table separation tests of the rough zircon concentrate.

Products	Yield/%	Grade/%		Recovery/%	
		TiO <sub>2</sub>	ZrO <sub>2</sub>	TiO <sub>2</sub>	ZrO <sub>2</sub>
Concentrate 1	13.91	5.76	40.47	2.96	17.04
Concentrate 2	32.69	14.02	43.58	16.89	43.13
Mixed concentrate	46.60	11.55	42.65	19.85	60.17
Tailing (Middling III)	53.40	40.72	24.64	80.15	39.83
Feeding	100.00	27.13	33.03	100.00	100.00

### 3.3.2. Tests for the Rough Rutile Concentrate

To further improve grade of the rough rutile concentrate obtained in Section 3.2.2, shaking table tests were carried out and the results were shown in Table 9. From the table, it is known that a rutile concentrate containing 53.76% TiO<sub>2</sub> was obtained with a TiO<sub>2</sub> recovery of 66.80% when the TiO<sub>2</sub> grade in the feeding was 51.50%. When the TiO<sub>2</sub> grade in the feeding increased to 56.06%, a rutile concentrate containing 61.75% TiO<sub>2</sub> was obtained with a TiO<sub>2</sub> recovery of 63.65%. These results indicated that the higher the TiO<sub>2</sub> grade in the feeding was, the better quality of concentrate was obtained. The reason is that the concentrate zone becomes wider on the surface of the shaking table when the feeding grade increases, while the tailings zone moves to the edge of the shaking table, thus increasing the concentrate grade [31]. Thus, the amounts of other minerals entering the following drying and electric separation will be reduced, resulting in an excellent separation performance and saving energy. These results further supported the conclusions obtained in Section 3.2.2. In addition, the TiO<sub>2</sub> grade in the tailing (Middling II) was 48.27%, that is, the tailing can be returned to the feeding of second-stage spiral chute to further recover rutile.

**Table 9.** Results of shaking table separation tests of the rough rutile concentrate.

Products	Yield/%	Grade/%		Recovery/%	
		TiO <sub>2</sub>	ZrO <sub>2</sub>	TiO <sub>2</sub>	ZrO <sub>2</sub>
Concentrate	58.65	53.76	6.99	66.80	83.28
Tailing (Middling II)	41.35	46.20	1.99	33.20	16.72
Feeding	100.00	51.50	4.92	100.00	100.00
Concentrate	57.78	61.75	7.01	63.65	81.75
Tailing (Middling II)	42.22	48.27	2.14	34.35	18.25
Feeding	100.00	56.06	4.95	100.00	100.00

### 3.3.3. Tests for the Tailing I

To further improve the recovery of TiO<sub>2</sub>, shaking table tests were tried to treat the tailing I which was obtained in the first-stage spiral chute (Section 3.2.1). The results are shown in Table 10. From Table 10, a rutile product (Middling IV) assaying 57.50% TiO<sub>2</sub> was obtained with a recovery of 89.22%, that is, the product can be returned to the feeding of the shaking table for the rough rutile concentrate. On the other hand, the tailing containing 3.29% TiO<sub>2</sub> and 0.07% ZrO<sub>2</sub> was directly discarded in the final tailing.

**Table 10.** Results of shaking table separation tests of the tailing I.

Products	Yield/%	Grade/%		Recovery/%	
		TiO <sub>2</sub>	ZrO <sub>2</sub>	TiO <sub>2</sub>	ZrO <sub>2</sub>
Concentrate (Middling IV)	28.72	57.50	0.72	89.22	80.56
Tailing	71.28	3.29	0.07	12.43	19.44
Feeding	100.00	18.86	0.26	100.00	100.00

### 3.4. Products Phase Analyses

To further ascertain the mineral composition of each product obtained by the shaking tables, XRD analyses were carried out and the results are shown in Figure 6. From (a), the signals of zircon diffraction peaks were significantly obvious although few of signals of rutile diffraction peaks also appeared. This further agreed with the results obtained in Table 8. From (b), it is seen that the rutile concentrate was composed of rutile (mainly) and zircon. On the other hand, signals of the diffraction peaks seemed to be weak. These results further confirmed that the raw sample was classified as an altered placer. From (c), it is known that the Middling IV was mainly composed of quartz and rutile. It was interesting that the peak intensity of quartz was higher than that of rutile. This may be accounted by the fact that the rutile was an altered product of the ilmenite in the beach placer, resulting in a bad crystal structure. From (d), it is found that the tailing was mainly composed of quartz, indicating that the shaking table could achieve an excellent removal of gangue.

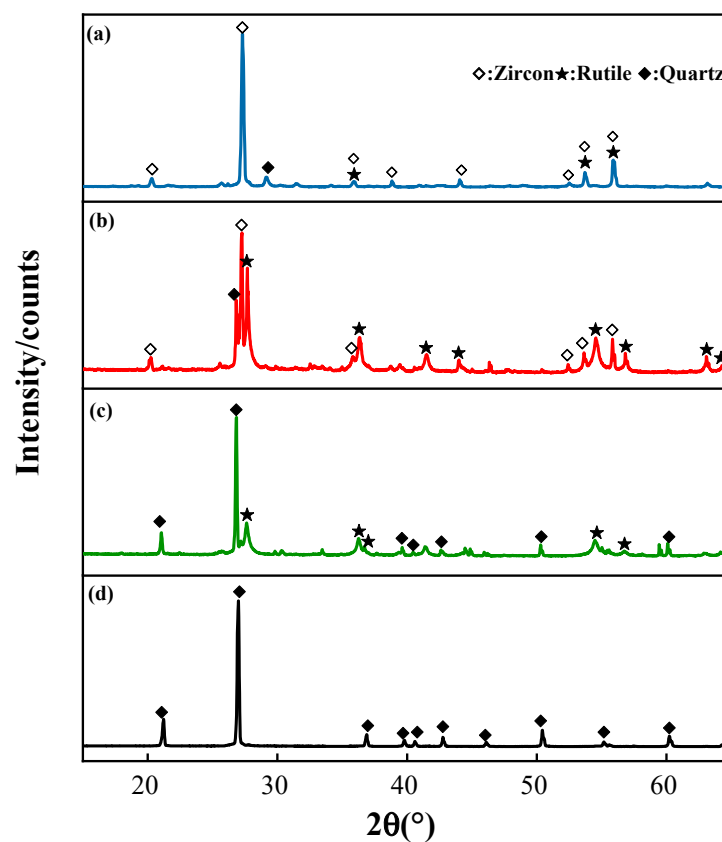


**Figure 6.** XRD pattern of the (a) zircon concentrate; (b) rutile concentrate; (c) middling IV; (d) Tailing.

### 3.5. Recommend Closed-Circuit Process

According to the above results, a closed-circuit beneficiation process which was mainly composed of spiral chutes and shaking tables was proposed to treat the complex rutile ore in the subsequent industrial production, as shown in Figure 7. The object was to increase the grade of  $ZrO_2$  and  $TiO_2$  in their respective concentrate as high as possible, which was beneficial for the following drying and electric separation and finally for achieving saving energy and cost reduction. In addition, the intermediate product was returned to the previous level separation operation which had approximate content of  $TiO_2$  or  $ZrO_2$  to from a closed cycle, resulting in an increase in the final recoveries of  $ZrO_2$  and  $TiO_2$ . It was believed that the complex rutile ore will be comprehensively and effectively utilized by the gravity separation.

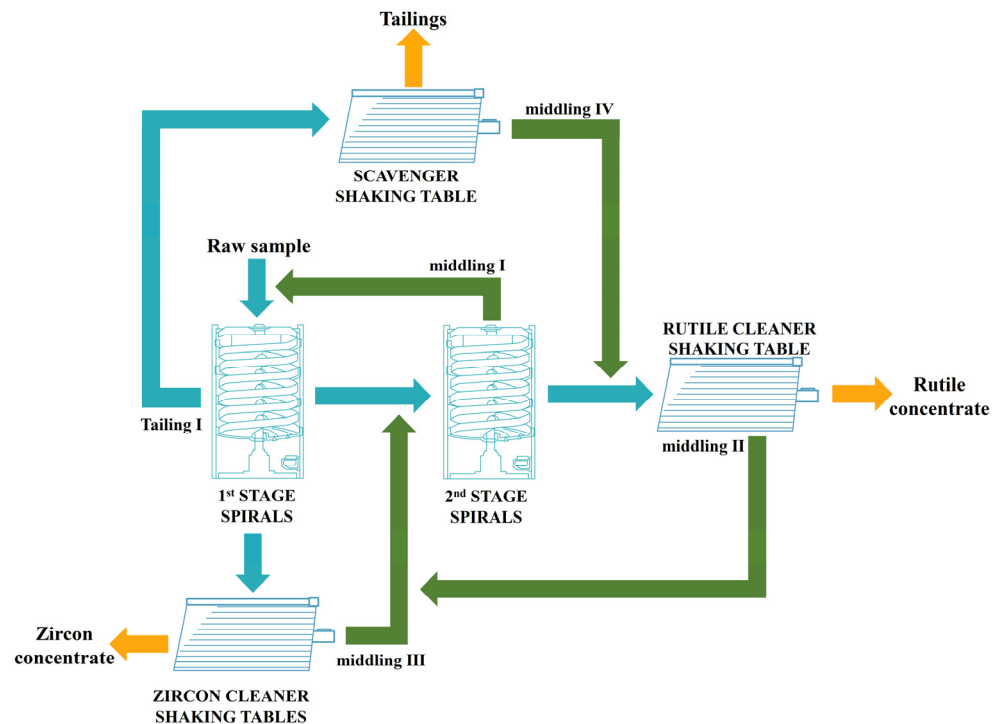


Figure 7. Recommend closed-circuit process.

#### 4. Conclusions

This paper investigated the mineralogy and gravity separation tests of the complex rutile ore. The important conclusions were drawn as follows:

(1) The raw sample assaying  $\text{TiO}_2$ : 33.78% and  $\text{ZrO}_2$ : 4.62% presented a high recovery value. The main components included rutile, iron-bearing rutile, zircon, ilmenite, quartz and Mg-Al spinel. The content of iron in most of rutile particles varied from 0% to 2.5%, which confirmed that the sample had a relatively complete alteration. The rutile and zircon in the raw sample presented a good liberation, which was advantageous for the subsequent separation and purification.  $\text{TiO}_2$  was mainly enriched in the particle size of  $-0.15$  mm and the distributions reached 95.17%. And zirconium dioxide was mainly enriched in the particle size of  $-0.106$  mm and the distribution reached 86.72%. The distribution of  $\text{TiO}_2$  and  $\text{ZrO}_2$  in the particle size of  $-0.074$  mm reached 32.08% and 52.25%, respectively, indicating that the valuable metal minerals were mainly distributed in fine particles.

(2) Two stages of spiral chute separation were firstly carried out to treat the complex rutile ore. It was found that the zone width of products which were removed at the port obviously affected the separation performance. After the first-stage spiral chute,  $\text{ZrO}_2$  and  $\text{TiO}_2$  grade in their products increased from 5.72% to 33.18% and from 33.56% to 43.52%, respectively. After the second-stage spiral chute,  $\text{TiO}_2$  grade in the product further increased to 56.77%;

(3) Shaking table tests were performed to improve the grade and recovery of  $\text{ZrO}_2$  and  $\text{TiO}_2$  in the products obtained by spiral chutes. After their respective tests,  $\text{ZrO}_2$  grade in the zirconium concentrate and  $\text{TiO}_2$  grade in the rutile concentrate increased to 42.65% and 61.75%, respectively. For the tailing of the first-stage spiral chute, a rutile product assaying 57.50%  $\text{TiO}_2$  was obtained with a recovery of 89.22% after the shaking table and the tailing was directly discarded as the final tailing. The XRD results of the products further illustrated that the mineral composition of each product obtained by the shaking tables and even revealed that the zircon, rutile and gangue were distributed from the inside to the outside on the bed of spiral chute and shaking table. Finally, a closed-circuit beneficiation process was proposed to treat the complex rutile ore for achieving comprehensive and effective utilization.

**Author Contributions:** Conceptualization, Z.W. and Y.Z.; methodology, Z.W., Y.Z. and X.H.; formal analysis, Z.W. and Y.Z.; resources, X.H. and X.W.; data curation, Z.W. and Y.Z.; writing—original draft preparation, Z.W.; writing—review and editing, Y.Z.; supervision, Y.Z., J.P. and Z.D.; All authors have read and agreed to the published version of the manuscript.

**Funding:** This research was supported by Science and Technology Major Project of Yunnan Province (No. 202202AG050007) and Maoming’s 2021 provincial science and technology innovation strategy “big project + task list” project (No. 2021S0005).

**Data Availability Statement:** No new data were created or analyzed in this study.

**Acknowledgments:** Samples are provided by the industrial sponsor Guangdong Ubridge New Material Technology Co., Ltd., Maoming, China.

**Conflicts of Interest:** Author Xiang Huang and Xiangding Wang were employed by the company Guangdong Ubridge New Material Technology Co., Ltd. The remaining authors declare that the research was conducted in the absence of any commercial or financial relationships that could be construed as a potential conflict of interest.

## References

1. Jackson, M.; Dring, K. A review of advances in processing and metallurgy of titanium alloys. *Mater. Sci. Technol* **2013**, *22*, 881–887. [[CrossRef](#)]
2. Feng, E.; Gao, D.; Wang, Y.; Yu, F.; Wang, C.; Wen, J.; Gao, Y.; Huang, G.; Xu, S. Sustainable recovery of titanium from secondary resources: A review. *J. Environ. Manag.* **2023**, *339*, 117818. [[CrossRef](#)] [[PubMed](#)]
3. Meinhold, G. Rutile and its applications in earth sciences. *Earth Sci. Rev.* **2010**, *102*, 1–28. [[CrossRef](#)]
4. Veiga, C.; Davim, J.P.; Loureiro, A.J.R. Review on machinability of titanium alloys: The process perspective. *Rev. Adv. Mater. Sci* **2013**, *34*, 148–164.
5. Jones, G. *Mineral Sands: An Overview of the Industry*; Iluka Resources Limited: Capel, Australia, 2009.
6. Qiu, G.; Guo, Y. Current situation and development trend of titanium metal industry in China. *Int. J. Miner. Metall. Mater* **2022**, *29*, 599–610. [[CrossRef](#)]
7. Schulz, K.J.; DeYoung, J.H.; Seal, R.R., II; Bradley, D.C. (Eds.) *Critical Mineral Resources of the United States—Economic and Environmental Geology and Prospects for Future Supply*; U.S. Geological Survey: Reston, VA, USA, 2017.
8. El Khalloufi, M.; Drevelle, O.; Soucy, G. Titanium: An Overview of Resources and Production Methods. *Minerals* **2021**, *11*, 1425. [[CrossRef](#)]
9. Perks, C.; Mudd, G. Titanium, zirconium resources and production: A state of the art literature review. *Ore Geol. Rev.* **2019**, *107*, 629–646. [[CrossRef](#)]
10. Pownceby, M.I.; Sparrow, G.J.; Aral, H.; Smith, L.K.; Bruckard, W.J. Recovery and processing of zircon from Murray Basin mineral sand deposits. *Miner. Process. Extr. Metall.* **2015**, *124*, 240–253. [[CrossRef](#)]
11. Bedinger, B.G.M. *Zirconium and Hafnium*; U.S. Geological Survey: Reston, VA, USA, 2017.
12. Bisht, A.; Martinez-Alier, J. Coastal sand mining of heavy mineral sands: Contestations, resistance, and ecological distribution conflicts at HMS extraction frontiers across the world. *J. Ind. Ecol.* **2022**, *27*, 238–253. [[CrossRef](#)]
13. Zhu, X.; Geng, Y.; Gao, Z.; Tian, X.; Xiao, S.; Houssini, K. Investigating zirconium flows and stocks in China: A dynamic material flow analysis. *Resour. Policy* **2023**, *80*, 103139. [[CrossRef](#)]
14. Li, Z.; Chen, C. Development Status of Global Titanium Resources Industry. *Acta Geosci. Sin.* **2021**, *42*, 6.
15. Farjana, S.H.; Huda, N.; Mahmud, M.A.P.; Lang, C. Towards sustainable TiO<sub>2</sub> production: An investigation of environmental impacts of ilmenite and rutile processing routes in Australia. *J. Clean. Prod.* **2018**, *196*, 1016–1025. [[CrossRef](#)]
16. Poon, P.; Graham, I.T.; Liepa, E.A.C.; Cohen, D.R.; Pringle, I.J.; Burkett, D.A.; Privat, K. Mineral distribution and provenance of heavy mineral sands (zircon, ilmenite, rutile) deposits from the NW Murray Basin, far western NSW, Australia. *Aust. J. Earth Sci.* **2020**, *67*, 575–590. [[CrossRef](#)]
17. Gonçalves, C.; Braga, P. Heavy Mineral Sands in Brazil: Deposits, Characteristics, and Extraction Potential of Selected Areas. *Minerals* **2019**, *9*, 176. [[CrossRef](#)]
18. Laxmi, T.; Srikant, S.S.; Rao, D.S.; Rao, R.B. Beneficiation studies on recovery and in-depth characterization of ilmenite from red sediments of badlands topography of Ganjam District, Odisha, India. *Int. J. Min. Sci. Technol. IJMST* **2013**, *23*, 725–731. [[CrossRef](#)]
19. Rao, R.B. Recovery of Ilmenite and Other Heavy Minerals from Teri Sands (Red Sands) of Tamil Nadu, India. *J. Miner. Mater. Charact. Eng.* **2009**, *8*, 149–159.
20. Rejith, R.G.; Sundararajan, M. Combined magnetic, electrostatic, and gravity separation techniques for recovering strategic heavy minerals from beach sands. *Mar. Georesour. Geotechnol.* **2017**, *36*, 959–965. [[CrossRef](#)]
21. Dieye, M.; Thiam, M.M.; Geneyton, A.; Gueye, M. Monazite Recovery by Magnetic and Gravity Separation of Medium Grade Zircon Concentrate from Senegalese Heavy Mineral Sands Deposit. *J. Miner. Mater. Charact. Eng.* **2021**, *09*, 590–608. [[CrossRef](#)]

22. Fawzy, M.M.; Ghar, M.; Gaafar, I.M.; Shafey, A.; Diab, M.; Hussein, A.W. *Recovery of Valuable Heavy Minerals via Gravity and Magnetic Separation Operations from Diit Quaternary Stream Sediments, Southern Coast of the Red Sea, Egypt*; IOP Publishing Ltd.: Bristol, UK, 2022.
23. Bazin, C.; Sadeghi, M.; Renaud, M. An operational model for a spiral classifier. *Miner. Eng.* **2016**, *91*, 74–85. [[CrossRef](#)]
24. Boucher, D.; Deng, Z.; Leadbeater, T.W.; Langlois, R.; Waters, K.E. Speed analysis of quartz and hematite particles in a spiral concentrator by PEPT. *Miner. Eng.* **2016**, *91*, 86–91. [[CrossRef](#)]
25. Yıldırım Gülsoy, Ö.; Gülcan, E. A new method for gravity separation: Vibrating table gravity concentrator. *Sep. Purif. Technol.* **2019**, *211*, 124–134. [[CrossRef](#)]
26. Peng, H.; Li, G.; Hu, H.; Zhou, Z. Research Actuality and Prospect of Spiral Chute. *Jiangxi Nonferrous Met.* **2009**, *23*, 26–29.
27. Galvin, K.P.; Iveson, S.M. New challenges for gravity concentration and classification of fine particles. *Miner. Eng.* **2022**, *190*, 107888. [[CrossRef](#)]
28. Bing, Y. Industrial Production Application Research and Development on YunTin YXB New Type Fine Sand Table Concentrator. *Yunnan Metall.* **2020**, *49*, 27–30.
29. Nayak, A.; Jena, M.S.; Mandre, N.R. Application of Enhanced Gravity Separators for Fine Particle Processing: An Overview. *J. Sustain. Metall.* **2021**, *7*, 315–339. [[CrossRef](#)]
30. Izerdem, D.; Ergun, S.L. Investigation of the effects of particle size on the performance of classical gravity concentration equipment. *Miner. Process. Extr. Metall. Rev.* **2022**, 1–18. [[CrossRef](#)]
31. Manser, R.; Barley, R.; Wills, B. The shaking table concentrator—The influence of operating conditions and table parameters on mineral separation—The development of a mathematical model for normal operating conditions. *Miner. Eng.* **1991**, *4*, 369–381. [[CrossRef](#)]

**Disclaimer/Publisher’s Note:** The statements, opinions and data contained in all publications are solely those of the individual author(s) and contributor(s) and not of MDPI and/or the editor(s). MDPI and/or the editor(s) disclaim responsibility for any injury to people or property resulting from any ideas, methods, instructions or products referred to in the content.